

PolyFit: Polynomial-based Indexing Approach for Fast Approximate Range Aggregate Queries

Zhe Li¹, Tsz Nam Chan², Man Lung Yiu¹, Christian S. Jensen³

Hong Kong Polytechnic University¹, Hong Kong Baptist University², Aalborg University³
 richie.li@connect.polyu.hk, edisonchan@comp.hkbu.edu.hk, csmlyiu@comp.polyu.edu.hk, csj@cs.aau.dk

ABSTRACT

Range aggregate queries find frequent application in data analytics. In many use cases, approximate results are preferred over accurate results if they can be computed rapidly and satisfy approximation guarantees. Inspired by a recent indexing approach, we provide means of representing a discrete point dataset by continuous functions that can then serve as compact index structures. More specifically, we develop a polynomial-based indexing approach, called PolyFit, for processing approximate range aggregate queries. PolyFit is capable of supporting multiple types of range aggregate queries, including COUNT, SUM, MIN and MAX aggregates, with guaranteed absolute and relative error bounds. Experiment results show that PolyFit is faster and more accurate and compact than existing learned index structures.

ACM Reference Format:

Zhe Li¹, Tsz Nam Chan², Man Lung Yiu¹, Christian S. Jensen³. 2021. PolyFit: Polynomial-based Indexing Approach for Fast Approximate Range Aggregate Queries. In *Proceedings of 24th International Conference on Extending Database Technology (EDBT), Cyprus, Nicosia (EDBT2021)*, 13 pages.
<https://doi.org/10.1145/nnnnnnnn.nnnnnnnn>

1 INTRODUCTION

A *range aggregate query* [33] retrieves records in a dataset that belong to a given key range and then applies an aggregate function (e.g., SUM, COUNT, MIN, MAX) to a attribute of those records. Range aggregate queries are used in OLAP [33, 63] and data analytics applications, e.g., for outlier detection [66, 68], data visualization [20], and tweet analysis [49]. For example, network intrusion detection systems [68] utilize range COUNT queries to monitor a network for anomalous activities. In many application scenarios, users accept approximate results provided that (i) they can be computed quickly and (ii) they are sufficiently accurate (e.g., within 5% error). We target such applications and focus on error-bounded evaluation of range aggregate queries.

A recent indexing approach represents the values of attributes in a dataset by continuous functions, which then serve to enable compact index structures [23, 39]. When compared to traditional index structures, this approach is able to yield a smaller index size and faster response time. The existing studies [23, 39] focus on computing exact results for point and range queries on 1-dimensional data. In contrast, we conduct a **comprehensive study of approximate range aggregate queries, supporting many aggregate functions and multi-dimensional data**.

The idea that underlies our proposal for using functions to answer approximate range aggregate queries may be explained as follows. Consider a stock market index (e.g., the Hong Kong Hang Seng Index) at different time as a dataset \mathcal{D} consisting of records of the form (index value, timestamp), where the former is

our measure and the latter is our key that is used for specifying query ranges—see Figure 1(a). A user can find the average stock market index value in a specified time range $[l_q, u_q]$ by issuing a range SUM query (and divide by $u_q - l_q + 1$). We propose to construct the cumulative function of \mathcal{D} as shown in Figure 1(b). If we can approximate this function well by a polynomial function $\mathbb{P}(x)$ then the range SUM query can be approximated as $\mathbb{P}(u_q) - \mathbb{P}(l_q)$, which takes $O(1)$ time. As another example, the user may wish to find the maximum stock market index in a specified time range. The timestamped index values in \mathcal{D} can be modeled by the continuous function shown in Figure 1(c). Again, if we can approximate this function well using a polynomial function $\mathbb{P}(x)$ then the range MAX query can be answered quickly using mathematical tools, e.g., by applying differentiation to identify maxima in $\mathbb{P}(x)$.

Regarding the two-dimensional case, consider the dataset of tweets' locations as shown in Figure 9(a) in Section 6, where each data point has a longitude (as key 1) and a latitude (as key 2). Suppose that the user wishes to count the number of tweets in a geographical region. Our idea is to derive the cumulative count function shown in Figure 9(b), and then approximate this function with a polynomial function $\mathbb{P}(x_1, x_2)$ (of two variables). This enables us to answer a two-dimensional range COUNT query in $O(1)$ time.

Another difference between our work and existing studies [23, 39] is the types of functions used for approximation. Our proposal uses piecewise polynomial functions, rather than piecewise linear functions [23, 39]. As we will show in Section 4, using polynomial functions yields lower fitting errors than using linear functions. Thus, our proposal leads to smaller index size and faster queries.

The key technical challenges are as follows. (1) How to find polynomial functions with low approximation error efficiently? (2) How to answer range aggregate queries with error guarantees? (3) How to support common aggregate functions (e.g., COUNT, SUM, MIN, MAX) and multi-dimensional data?

To tackle these challenges, we develop the polynomial-based indexing approach (PolyFit) for processing approximate range aggregate queries. Our contributions are summarized as follows.

- To the best of our knowledge, this is the first study that utilizes polynomial functions to learn indexes that support approximate range aggregate queries.
- PolyFit supports multiple types of range aggregate queries, including COUNT, SUM, MIN and MAX with guaranteed deterministic absolute and relative error bounds.
- Experiment results show that PolyFit achieves significant speedups, compared with the closest related works [23, 39], and traditional exact/approximate methods. For instance, for the OpenStreetMap dataset with 100M records, our index occupies only 4 MBytes and offers 5 μ s query response time (per 2-dimensional range COUNT query).

The rest of the paper is organized as follows. We first review the related work in Section 2. Next, we introduce preliminaries in Section 3. Then, we present our index construction techniques in

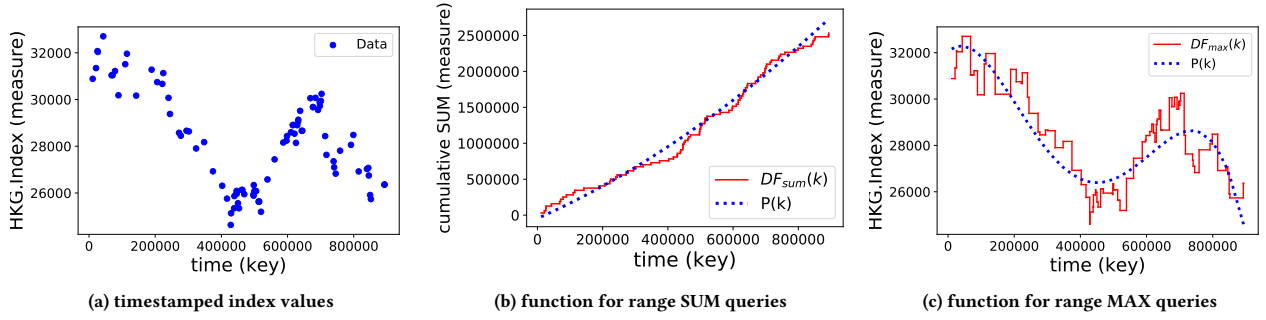


Figure 1: Stock market index values, 1-dimensional keys: discrete data points vs. continuous function

Section 4 and elaborate how to answer approximate range aggregate queries in Section 5. Next, we extend our idea for datasets with two keys in Section 6. Lastly, we present our experiments in Section 7 and conclude in Section 8.

2 RELATED WORK

Range aggregate queries are used frequently in analytics applications and constitute important functionality in OLAP and data warehousing [10, 11, 16, 19, 33, 35, 51, 63]. Exact solutions are based on prefix-sum arrays [33] or aggregate R-trees [54]. Due to the need for real-time performance in some applications (e.g., μ s-level response time [68]), many proposals exist that aim to improve the efficiency of range aggregate queries. These proposals can be classified as being either data-driven or query-driven. In addition, we also review some other studies, including learned index, and time series database, which are also related to this work.

Data-driven proposals build statistical models of a dataset for estimating query selectivity or the results of range aggregate queries. These models employ multi-dimensional histograms [34, 47, 52, 62], data sampling [8, 29, 31, 46, 55, 60], or kernel density estimation [27, 28, 32]. Although such proposals that compute approximate results are much faster than exact solutions, e.g., achieving ms (10^{-3}) level response time [56], they still do not offer real-time performance (e.g., μ s level [68]). Furthermore, these proposals do not offer theoretical approximation error guarantees.

The **query-driven approaches** utilize query workload to build statistical models of a dataset. Typical methods include error-feedback histograms [6, 9, 44], max-entropy histograms [50, 59], and learning-based model [48]. In addition, Park et al. [56] explore the approach of using mixture probabilistic models. These methods assume that new queries follow the historical query workload distribution. However, as a study [12] observes, this assumption may not always hold in practice. Further, even when this assumption is valid, the number of queries that are similar to those used for training may be much smaller if the queries follow a power law distribution [67], which can cause poor accuracy, and render it impossible to obtain useful approximation error guarantees for range aggregate queries.

Recently, **learning-based methods** have been used to construct more compact and effective index structure, that hold potential to accelerate database operations. Kraska et al. [39] propose the RMI index, which incorporates different machine learning models, e.g., linear regression and deep-learning, to improve the efficiency of range queries. Galakatos et al. [23] develop the FITing-tree, which is a segment-tree-like-structure [18, 65] that can significantly improve the efficiency of exact

point queries. Ferragina et al. [22] further support efficient update operations for range queries. Wang et al. [64] extend this learning-based approach to the spatial domain with their learned Z-order model that aims to support fast spatial indexing. However, there are two main differences between these proposals and our proposal. First, they either support range queries [22, 39, 64] or point queries [23], but not range aggregate queries. Second, we are the first to exploit polynomial functions to build index structures for approximate range aggregate queries.

In **time series database** community, there are also some research studies that utilize mathematical models to approximate time series data by a bunch of models. Representative approaches include piecewise linear approximation [36–38, 45], discrete wavelet transform [14, 57], discrete Fourier transform [21, 58], and their combinations [35, 53]. However, all of these studies either focus on the time-series similarity search (e.g., range or nearest neighbor queries) or time series compression problem, which are not designed to answer range aggregate queries in our context. Some of these studies also utilize the piecewise linear approximation [36, 37, 45], to approximate time-series, which is similar with our idea. In contrast, we achieve much better performance by utilizing some nonlinear (polynomial) functions to approximate the curve, which can reduce the number of segments dramatically. Furthermore, we can also support the segmentation of surface (e.g., Figure 9(b)), rather than only 1-D curve.

3 PRELIMINARIES

First, we define range aggregate queries and their approximate versions in Section 3.1. Then, we discuss the baselines for answering exact range aggregate queries in Section 3.2. Table 1 summarizes frequently used symbols in this paper.

Table 1: Symbols

Symbol	Description
\mathcal{D}	dataset
n	number of records in \mathcal{D}
R_{count}	range COUNT query
R_{sum}	range SUM query
R_{min}	range MIN query
R_{max}	range MAX query
CF_{sum}	cumulative function for range SUM query
DF_{max}	key-measure function for range MAX query
$\mathbb{P}(k)$	polynomial function
I	interval
deg	degree of polynomial function

3.1 Problem Definition

We focus on the setting that a range aggregate query specifies a *key* attribute (for range selection) and a *measure* attribute for aggregation. We shall consider the setting of two keys in Section 6. As such, the dataset \mathcal{D} is a set of $(key, measure)$ records, i.e., $\mathcal{D} = \{(k_1, m_1), (k_2, m_2), \dots, (k_n, m_n)\}$. For ease of presentation, we assume that key values are distinct and every m_i is non-negative. Then we define a range aggregate query below.

Definition 3.1. Let \mathcal{G} be an aggregate function on a measure attribute (e.g., COUNT, SUM, MIN, MAX). Given a dataset \mathcal{D} and a key range $[l_q, u_q]$, we express the result of a range aggregate query, in terms of relational algebra operations [7], as follows:

$$R_{\mathcal{G}}(\mathcal{D}, [l_q, u_q]) = \mathcal{G}(\sigma_{k \in [l_q, u_q]}(\mathcal{D})) \quad (1)$$

We aim to develop efficient methods for obtaining an approximate result of $R_{\mathcal{G}}(\mathcal{D}, [l_q, u_q])$ with two types of error guarantees [24, 25], namely the absolute error guarantee (cf. Problem 1) and the relative error guarantee (cf. Problem 2).

PROBLEM 1 (Q_{abs}). Given an absolute error ϵ_{abs} and a range aggregate query, we ask for an approximate result A_{abs} such that:

$$|A_{abs} - R_{\mathcal{G}}(\mathcal{D}, [l_q, u_q])| \leq \epsilon_{abs} \quad (2)$$

PROBLEM 2 (Q_{rel}). Given a relative error ϵ_{rel} and a range aggregate query, we ask for an approximate result A_{rel} such that:

$$\frac{|A_{rel} - R_{\mathcal{G}}(\mathcal{D}, [l_q, u_q])|}{R_{\mathcal{G}}(\mathcal{D}, [l_q, u_q])} \leq \epsilon_{rel} \quad (3)$$

3.2 Baselines: Exact Methods

We proceed to discuss exact methods for answering range SUM queries and range MAX queries. These methods can be easily extended to support COUNT and MIN respectively.

3.2.1 Exact method for range SUM queries. First, we define the key cumulative function as $CF_{sum}(k)$:

$$CF_{sum}(k) = R_{sum}(\mathcal{D}, [-\infty, k]) \quad (4)$$

The additive property of CF_{sum} enables us to compute the exact result of the range SUM query as:

$$R_{sum}(\mathcal{D}, [l_q, u_q]) = CF_{sum}(u_q) - CF_{sum}(l_q) \quad (5)$$

Then, we discuss how to obtain the terms $CF_{sum}(l_q)$ and $CF_{sum}(u_q)$ efficiently. Although CF_{sum} is a continuous function, it can be expressed by a discrete data structure with finite space. Specifically, we can presort the dataset \mathcal{D} in the ascending key order, then follow this order to construct a key-cumulative array of entries $(k, CF_{sum}(k))$. At query time, the terms $CF_{sum}(l_q)$ and $CF_{sum}(u_q)$ can be obtained by performing binary search on the above key-cumulative array. This step takes $O(\log n)$ time.

As a remark, this key-cumulative array is similar to the prefix-sum array [33]. The difference is that our array allows floating-point search key, while the prefix-sum array does not.

3.2.2 Exact method for range MAX queries. First, we define the following key-measure function $DF_{max}(k)$ (cf. Equation 6) to capture the data distribution in the dataset \mathcal{D} . An example of function $DF_{max}(k)$ is shown in Figure 2(a).

$$DF_{max}(k) = \begin{cases} \vdots & \vdots \\ m_i & \text{if } k_i \leq k < k_{i+1} \\ m_{i+1} & \text{if } k_{i+1} \leq k < k_{i+2} \\ \vdots & \vdots \\ 0 & \text{otherwise} \end{cases} \quad (6)$$

An aggregate max-tree [54] (cf. Figure 2(b)) can be built to answer range MAX queries. In this tree, each internal node covers an interval and stores the maximum measure within that interval. We then discuss how to process the query $R_{max}(\mathcal{D}, [l_q, u_q])$, whose query range is indicated by the red line in Figure 2(a). In Figure 2(b), we start from the root of the tree and explore its children, i.e., N_1 and N_2 . If a node (e.g., N_1) partially intersects with the query range, we visit its child nodes (e.g., N_3, N_6). When the interval of a node (e.g., N_4, N_5) is covered by the query range, we directly use its stored aggregate value without visiting its child nodes. During the traversal process, we keep track of the maximum measure seen so far. This procedure takes $O(\log n)$ time as we check at most two branches per level.

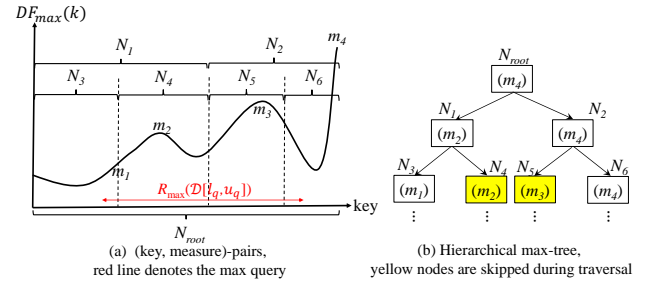


Figure 2: Aggregate MAX tree

4 INDEX CONSTRUCTION

Traditional index structures (e.g., B-tree [17]) need to store n keys, where n is the cardinality of the dataset \mathcal{D} . Thus, the index size grows linearly with the data size. To reduce the index size dramatically, we plan to index a limited number of functions (instead of n keys).

As a case study, we compare existing fitting functions [23, 39] with our fitting function (polynomial) on a real dataset (the Hong Kong 40-Index in 2018 [3]) in Figure 3. The exact key-measure function $DF_{max}(k)$ exhibits a complex shape. Observe that linear functions, e.g., linear regression $LR(k)$ [39] and linear segment $FIT(k)$ [23], cannot accurately approximate the exact function. In this paper, we adopt the polynomial function $\mathbb{P}(k)$, which can capture the nonlinear property¹ and achieve better approximation of $DF_{max}(k)$. In this example, $\mathbb{P}(k)$ is a degree-4 polynomial function (blue dotted line).

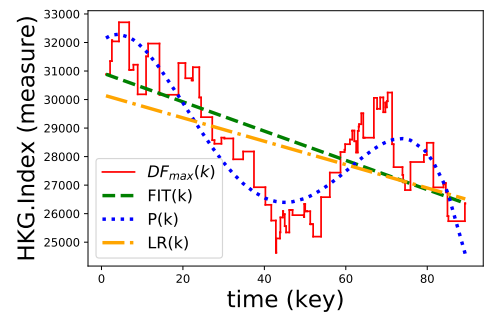


Figure 3: Curve fitting of Hong Kong 40-Index in 2018 [3]

¹As a remark, other types of nonlinear functions (e.g., logarithmic function, and trigonometric function etc.) require higher computation cost than polynomial function. Thus, we leave other types of nonlinear functions as our future work.

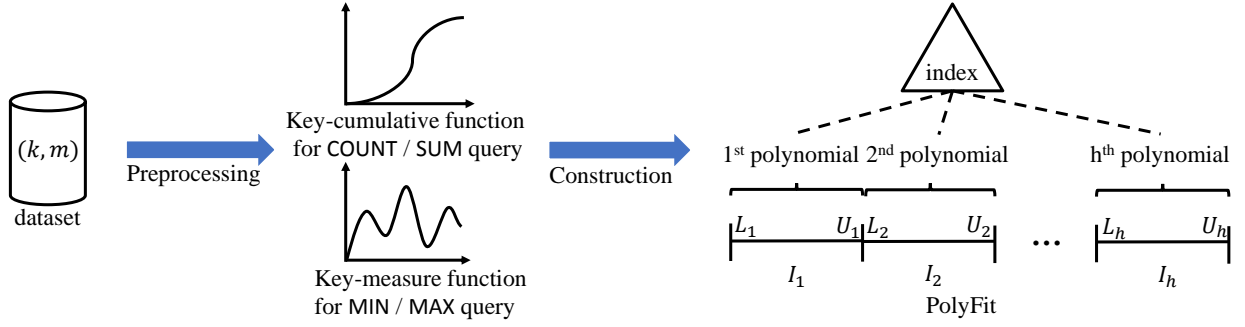


Figure 4: Indexing framework for PolyFit, each leaf entry stores a polynomial function

We introduce our indexing framework in Figure 4. First, we convert the dataset into the following exact function $F(k)$ based on the aggregate function \mathcal{G} and the functions in Section 3.2.

$$F(k) = \begin{cases} CF_{sum}(k), & \text{if } \mathcal{G} = \text{SUM} \\ DF_{max}(k), & \text{if } \mathcal{G} = \text{MAX} \end{cases} \quad (7)$$

We plan to compute an error-bounded approximation of $F(k)$ by using a sequence of polynomial functions. In Section 4.1, we examine how to find the best polynomial fitting of $F(k)$ in a given key interval I . Then, in Section 4.2, we propose a segmentation method for $F(k)$ in order to minimize our index size subject to a given deviation threshold. Finally, in Section 4.3, we discuss how to build an index for a sequence of polynomial functions.

4.1 Polynomial Fitting in a Key Interval

We shall discuss how to find the best fitting polynomial function of $F(k)$ in a given key interval I . First, we express a polynomial function $\mathbb{P}(k)$ as follows:

$$\mathbb{P}(k) = \sum_{j=0}^{deg} a_j k^j \quad (8)$$

where deg is the degree and each a_j is a coefficient. Note that the choice of deg entails tradeoffs between the fitting error and the online query evaluation cost. We will discuss the choice of deg in Section 5.3.

We formulate the following optimization problem in order to minimize the fitting error between $\mathbb{P}(k)$ and $F(k)$.

Definition 4.1. Let $F(k)$ be the exact function and I be a given key interval. Let k_1, k_2, \dots, k_ℓ be the keys of \mathcal{D} in interval I . We aim to find polynomial coefficients, a_0, a_1, \dots, a_{deg} that minimize the following error:

$$E(I) = \min_{a_0, a_1, \dots, a_{deg} \in \mathbb{R}} \max_{1 \leq i \leq \ell} |F(k_i) - \mathbb{P}(k_i)| \quad (9)$$

This is equivalent to the following linear programming problem, where the coefficients a_0, a_1, \dots, a_{deg} and t are variables.

$$\begin{cases} \text{MINIMIZE } t \\ \text{SUBJECT TO:} \\ -t \leq F(k_1) - (a_{deg}k_1^{deg} + \dots + a_2k_1^2 + a_1k_1 + a_0) \leq t \\ -t \leq F(k_2) - (a_{deg}k_2^{deg} + \dots + a_2k_2^2 + a_1k_2 + a_0) \leq t \\ \dots \\ -t \leq F(k_\ell) - (a_{deg}k_\ell^{deg} + \dots + a_2k_\ell^2 + a_1k_\ell + a_0) \leq t \\ \forall a_i \in \mathbb{R} \end{cases} \quad (10)$$

It takes $O(\ell^{2.5})$ time to solve the above linear programming problem (Equation 10) [41]. In our experimental study, we adopt

the IBM CPLEX linear programming library as the LP Solver, which is believed to be the most reliable and efficient among other implementations [26]. We will discuss some subtle issues like precision limitations in Section 5.3.

4.2 Minimal Index Size with Bounded Error

To support approximate query evaluation (in Section 5), we require that the fitting polynomial functions should satisfy a given error constraint. However, a single polynomial function is unlikely to fit accurately for the entire key domain. Thus, we propose to partition the key domain into intervals I_1, I_2, \dots, I_h so that each interval I_i satisfies the following requirement:

$$E(I) \leq \delta$$

where δ is a given deviation threshold. For instance, in Figure 5, the key domain is partitioned into two intervals I_1 and I_2 so that the best fitting polynomial function in each interval satisfies the error requirement.

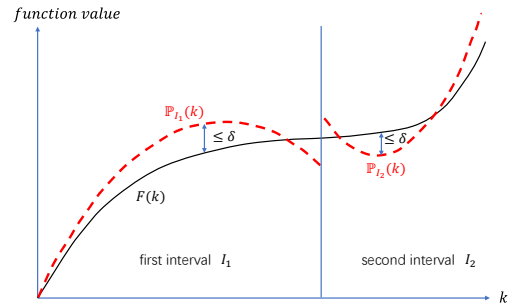


Figure 5: Fitting $F(k)$ with multiple polynomial functions, subject to the deviation threshold δ

To achieve a small index size, we aim to minimize the number of intervals (i.e., h in Figure 4). The dynamic programming (DP) approach [42], though designed for piecewise linear functions, can be adapted to solve our partitioning problem of $F(k)$. However, this method takes $O(n^2 \times \ell_{max}^{2.5})$ time², where ℓ_{max} is the maximum number of keys covered by any interval. Obviously, this method does not scale well with the data size n .

In Section 4.2.1, we present a more efficient method, called greedy segmentation (GS), to segment the exact function $F(k)$. As we will show later, the time complexity of GS is $O(n \times \ell_{max}^{2.5})$, which scales well with the data size n . Then, in Section 4.2.2, we show that GS is guaranteed to return the optimal solution.

²Recall that the state-of-the-art linear programming solver [41] takes $O(\ell_{max}^{2.5})$ time for each curve-fitting problem (cf. Equation 10).

4.2.1 Greedy Segmentation (GS) Method. We present the pseudo-code of the Greedy Segmentation (GS) method in Algorithm 1. It examines the key domain from left to right (line 2). In each iteration, it expands the interval I by including the next key (line 3), calls LP solver on the interval I to obtain a fitting function \mathbb{P}_{now} (line 4), and tests whether it fulfills the error requirement. When this test fails (i.e., $E(I) > \delta$), we conclude that the previous interval is a maximal interval and thus insert its corresponding fitting function \mathbb{P}_{prev} into the result. The above procedure is repeated until all keys are covered.

Algorithm 1 Greedy Segmentation (GS)

Input: function $F(k)$, degree deg , deviation threshold δ
Output: sequence of polynomial functions $\text{Seq}_{\mathbb{P}}$

```

1:  $\text{Seq}_{\mathbb{P}} \leftarrow \emptyset$ ;  $l \leftarrow 1$ ;  $\mathbb{P}_{prev} \leftarrow null$ 
2: for  $u \leftarrow 2$  to  $n$  do
3:    $I \leftarrow [k_l, k_u]$  ▷ the interval for polynomial function  $\mathbb{P}$ 
4:    $\mathbb{P}_{now} \leftarrow$  call LP solver on  $I$  ▷ Equation 10
5:   if  $E(I) > \delta$  or  $u = n$  then ▷ Equation 9
6:     insert  $\mathbb{P}_{prev}$  into  $\text{Seq}_{\mathbb{P}}$ 
7:      $l \leftarrow u$ 
8:    $\mathbb{P}_{prev} \leftarrow \mathbb{P}_{now}$ 
9: return  $\text{Seq}_{\mathbb{P}}$ 

```

The time complexity of GS is $O(n\ell_{max}^{2.5})$ because it invokes $O(n)$ calls to LP solver and each LP solver call takes $O(\ell_{max}^{2.5})$ time [41]. We further accelerate GS by applying the exponential search technique [13], which can reduce the number of LP calls per interval by $\frac{\ell}{\log \ell}$ times. With this technique, GS takes only 70 seconds (cf. Section 7.2.2) to complete for a real dataset with 1 million data points. This is acceptable for many data analytics tasks (with static datasets) in OLAP. In our experiments, we find that ℓ_{max} usually ranges between hundreds and thousands, thus the term $O(\ell_{max}^{2.5})$ is acceptable in practice.

4.2.2 GS is Optimal. We first prove the following property (Lemma 4.2) of our curve fitting problem (cf. Definition 4.1).

LEMMA 4.2. *Let I_l and I_u be two intervals, which contain two sets of keys S_l and S_u respectively. If $S_l \subseteq S_u$, then $E(I_l) \leq E(I_u)$.*

PROOF. Recall that the value of $E(I)$ (cf. Equation 9) is equal to the minimum value of the optimization problem (Equation 10). Since the S_l is a subset of S_u , the set of constraints for solving $E(I_l)$ is also the subset of constraints for solving $E(I_u)$. Thus, for the minimizing problem in Equation 10, the possible solution space for S_l is a superset of the possible solution space for S_u . Therefore, we conclude that $E(I_l) \leq E(I_u)$. \square

Based on Lemma 4.2, we then show that GS produces the fewest polynomial functions (cf. Theorem 4.3), i.e., the optimal solution.

THEOREM 4.3. *GS always produces the optimal number of functions (with respect to the given parameters deg and δ).*

PROOF. Let $\mathcal{I}_{OPT}^* = (I_{OPT}^{(1)}, I_{OPT}^{(2)}, \dots)$ and $\mathcal{I}_{GS}^* = (I_{GS}^{(1)}, I_{GS}^{(2)}, \dots)$ be two ascending sequences of intervals for the optimal solution and our GS method respectively. Every interval I in \mathcal{I}_{OPT}^* and \mathcal{I}_{GS}^* must satisfy $E(I) \leq \delta$. We denote the minimum key and the maximum key of $I_{algo}^{(i)}$ by $I_{algo}^{(i)}.k_{min}$ and $I_{algo}^{(i)}.k_{max}$, respectively.

Since both GS and OPT must cover the key domain, we have:

$$I_{GS}^{(1)}.k_{min} = I_{OPT}^{(1)}.k_{min}$$

According to GS, the first interval $I_{GS}^{(1)}$ is maximal in length, because a larger interval would violate the deviation threshold δ . Thus, we have:

$$I_{GS}^{(1)}.k_{max} \geq I_{OPT}^{(1)}.k_{max} \quad (11)$$

Together with the fact that \mathcal{I}_{OPT}^* and \mathcal{I}_{GS}^* are ascending sequences of intervals, we get:

$$I_{GS}^{(2)}.k_{min} \geq I_{OPT}^{(2)}.k_{min} \quad (12)$$

Then, we consider two cases for comparing $I_{GS}^{(2)}$ and $I_{OPT}^{(2)}$.

Case 1:

$$I_{GS}^{(2)}.k_{max} \geq I_{OPT}^{(2)}.k_{max}$$

In this case, the first two intervals of GS cover all keys in the first two intervals of OPT.

Case 2:

$$I_{GS}^{(2)}.k_{max} < I_{OPT}^{(2)}.k_{max} \quad (13)$$

Consider the interval $I' = [I_{GS}^{(2)}.k_{min}, I_{OPT}^{(2)}.k_{max}]$. By using Equations 12 and 13, we obtain: $I' \subset I_{OPT}^{(2)}$. By Lemma 4.2, we get: $E(I') \leq E(I_{OPT}^{(2)})$. Since $E(I_{OPT}^{(2)}) \leq \delta$, we get: $E(I') \leq \delta$.

Observe that I' has the same minimum key as $I_{GS}^{(2)}$ but a larger maximum key than $I_{GS}^{(2)}$. Since I' could not pass the error test in GS, it means that $E(I') > \delta$. This contradicts with an aforementioned statement ($E(I') \leq \delta$).

The above argument can be applied to any integer ℓ :

$$I_{GS}^{(\ell)}.k_{max} \geq I_{OPT}^{(\ell)}.k_{max}$$

which means the first ℓ intervals of GS cover all keys in the first ℓ intervals of OPT. Thus, we claim that GS produces the optimal number of functions. \square

4.3 Indexing of polynomial functions

In our experimental study, the number of intervals (for polynomial functions) range from 100 to 1000. We adopt existing index structures on these intervals to support fast query evaluation. Specifically, we employ an in-memory index called STX B-tree [4] to index intervals. For MAX (MIN) query, we maintain an extra aggregate max (min) attribute in each internal node to boost the query performance.

5 APPROXIMATE QUERY EVALUATION

We present our framework for answering approximate range aggregate queries in Figure 6. The first step is to compute an initial approximate result quickly by using our index (PolyFit). Then, we check whether the error condition is satisfied, and refine the approximate result if necessary. We then discuss how to answer the approximate range SUM query and the approximate range MAX query in Sections 5.1 and 5.2, respectively. Finally, in Section 5.3, we discuss how to tune our index parameters (e.g., deg, δ) in order to optimize the query response time.

5.1 Approximate range SUM Query

Given the query range $[l_q, u_q]$, we propose to compute the approximate result as:

$$\tilde{A}_{sum} = \mathbb{P}_{I_u}(u_q) - \mathbb{P}_{I_l}(l_q) \quad (14)$$

where I_l and I_u denote the intervals of \mathbb{P} that l_q and u_q overlap, which could be found using the index mentioned in Section 4.3.

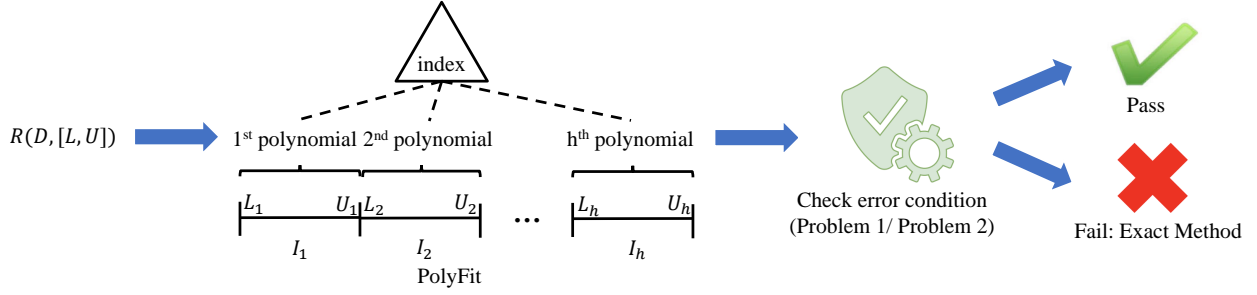


Figure 6: Querying framework for PolyFit

Then, we show the error conditions for Q_{abs} (cf. Problem 1) and Q_{rel} (cf. Problem 2).

Error condition for Q_{abs}

Given the absolute error ϵ_{abs} , we recommend to use the deviation threshold $\delta = \frac{\epsilon_{abs}}{2}$ in constructing PolyFit. With this setting, the following lemma offers the absolute error guarantee for the approximate result \tilde{A}_{sum} (in Equation 14).

LEMMA 5.1. *If $\delta = \frac{\epsilon_{abs}}{2}$, then \tilde{A}_{sum} (in Equation 14) satisfies the absolute error guarantee of ϵ_{abs} .*

PROOF. Let I_l and I_u be two intervals (in PolyFit) which contain l_q and u_q (of the query range $[l_q, u_q]$) respectively. Based on the deviation threshold guarantee in Section 4.2.2, we obtain:

$$|CF_{sum}(l_q) - \mathbb{P}_{I_l}(l_q)| \leq \delta$$

$$|CF_{sum}(u_q) - \mathbb{P}_{I_u}(u_q)| \leq \delta$$

By combining them, we have:

$$CF_{sum}(u_q) - CF_{sum}(l_q) - 2\delta \leq \tilde{A}_{sum} \leq CF_{sum}(u_q) - CF_{sum}(l_q) + 2\delta$$

By using Equation 5, we have:

$$R_{sum}(\mathcal{D}, [l_q, u_q]) - 2\delta \leq \tilde{A}_{sum} \leq R_{sum}(\mathcal{D}, [l_q, u_q]) + 2\delta$$

Since $\delta = \frac{\epsilon_{abs}}{2}$, \tilde{A}_{sum} satisfies the absolute error guarantee ϵ_{abs} . \square

Error condition for Q_{rel}

In this scenario, this is no specific preference for setting the deviation threshold δ in constructing PolyFit. The following lemma suggests a condition to test whether \tilde{A}_{sum} satisfies the relative error guarantee. If this test fails, we resort to the exact method (cf. Section 3.2.1) to obtain the exact result.

LEMMA 5.2. *If $\frac{2\delta}{\tilde{A}_{sum} - 2\delta} \leq \epsilon_{rel}$, then \tilde{A}_{sum} (in Equation 14) satisfies the relative error guarantee of ϵ_{rel} .*

PROOF. According to Lemma 5.1, we have:

$$|\tilde{A}_{sum} - R_{sum}(\mathcal{D}, [l_q, u_q])| \leq 2\delta \quad (15)$$

By rearranging terms, we obtain:

$$R_{sum}(\mathcal{D}, [l_q, u_q]) \geq \tilde{A}_{sum} - 2\delta \quad (16)$$

By dividing Equation 15 with Equation 16, we can achieve the following relative error.

$$\frac{|\tilde{A}_{sum} - R_{sum}(\mathcal{D}, [l_q, u_q])|}{R_{sum}(\mathcal{D}, [l_q, u_q])} \leq \frac{2\delta}{\tilde{A}_{sum} - 2\delta}$$

Since $\frac{2\delta}{\tilde{A}_{sum} - 2\delta} \leq \epsilon_{rel}$, \tilde{A}_{sum} satisfies the relative error guarantee. \square

The overall query algorithm

We summarize the query algorithm for both types of error guarantees in Algorithm 2. The processing for Q_{abs} is composed of two parts: index search T_1 (i.e., Lines 1-2) and function evaluation T_2 (i.e., Line 3). The processing for Q_{rel} includes T_1 , T_2 , and possible refinement T_3 (i.e., Lines 4-6). The time complexity of T_1 , T_2 , and T_3 are $O(\log(|Seq_P|))$, $O(deg)$, and $O(\log |D|)$ respectively.

Algorithm 2 Query Processing for SUM (or COUNT)

Input: $Seq_P, l_q, u_q, \mathcal{D}, \delta, Q_{type}$

Output: Approximate query result A

- 1: $\mathbb{P}_{I_l} \leftarrow$ index search \mathbb{P} from Seq_P that cover l_q
- 2: $\mathbb{P}_{I_u} \leftarrow$ index search \mathbb{P} from Seq_P that cover u_q
- 3: $\tilde{A}_{sum} \leftarrow \mathbb{P}_{I_u}(u_q) - \mathbb{P}_{I_l}(l_q)$
- 4: **if** $Q_{type} = Q_{rel}$ **then**
- 5: **if** \tilde{A}_{sum} fails the error condition of Lemma 5.2 **then**
- 6: $\tilde{A}_{sum} \leftarrow$ perform refinement on \mathcal{D} ▷ Section 3.2.1
- 7: **return** \tilde{A}_{sum}

5.2 Approximate range MAX Query

Given the query range $[l_q, u_q]$, we propose to compute the approximate result as:

$$\tilde{A}_{max} = \max \left\{ \max_{k \in I_l, k \geq l_q} \mathbb{P}_{I_l}(k), \max_{k \in I_u, k \leq u_q} \mathbb{P}_{I_u}(k), \max_{N_j, I \subseteq [l_q, u_q]} N_j.max \right\} \quad (17)$$

where N_j denotes the internal node of the index built on top of Seq_P . I_l and I_u denote the intervals of \mathbb{P} that l_q and u_q overlap in the leaf nodes.

The error conditions for Q_{abs} and Q_{rel} are presented in Lemmas 5.3) and 5.4) respectively. We omit their proofs; they are similar to the proofs of Lemmas 5.1 and 5.2.

LEMMA 5.3. *If $\delta = \epsilon_{abs}$, then \tilde{A}_{max} (in Equation 17) satisfies the absolute error guarantee ϵ_{abs} .*

LEMMA 5.4. *If $\tilde{A}_{max} \geq \delta(1 + \frac{1}{\epsilon_{rel}})$, then \tilde{A}_{max} (in Equation 17) satisfies the relative error guarantee ϵ_{rel} .*

We now discuss how to evaluate Equation 17. The third term is contributed by the inner nodes of aggregate R-tree whose intervals are covered by $[l_q, u_q]$. Regarding the first two terms, it suffices to find the maximum values for $\mathbb{P}_{I_l}(k)$ and $\mathbb{P}_{I_u}(k)$ in regions $[l_q, U_{I_l}]$ and $[L_{I_u}, u_q]$, as shown in Figure 7. These values (i.e., red dots) can be calculated by checking the border points and the zero derivative points.

The overall query algorithm

We conclude the query algorithm for both types of error guarantees in Algorithm 3. It uses an aggregate R-tree built on top of

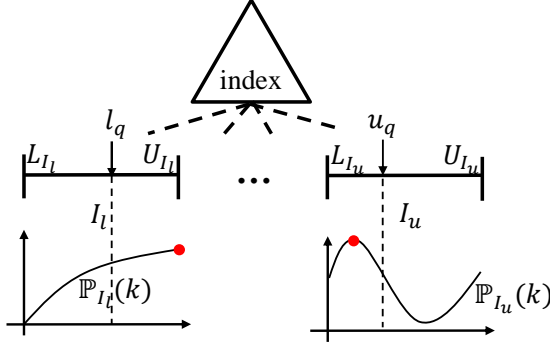


Figure 7: The maximum measure values (red dots) for two leaf nodes, which include l_q and u_q

polynomial functions. The processing for Q_{abs} consists of two parts: index search T_1 (i.e., Line 3) and function evaluation T_2 (Lines 8-9). The processing for Q_{rel} includes T_1 , T_2 , and possible refinement T_3 (i.e., Lines 10-12). The time complexity of T_1 and T_3 are still $O(\log(|\text{Seq}_{\mathbb{P}}|))$ and $O(\log |\mathcal{D}|)$. However, for T_2 , this includes calculating the zero derivative points within the intersection region. If the degree is between 1 and 5, there exist closed-form equations, where the number of arithmetic operations in these cases are summarized in Table 2. Starting from degree 6, there is no closed-form equations, and thus require expensive numerical evaluation methods like gradient descent [61]. In practice, we recommend to use the degree up to 3 for approximate range MAX query.

Algorithm 3 Query Processing for MAX (or MIN)

Input: Aggregate R-tree N on $\text{Seq}_{\mathbb{P}}$, l_q , u_q , \mathcal{D} , δ , Q_{type}

Output: Approximate query result A

```

1:  $\tilde{A}_{max} \leftarrow -\infty$ 
2: if  $N$  is an internal node then
3:   update  $\tilde{A}_{max}$  based on aggregate R-tree's mechanism
4: else
5:   for leaf element  $\mathbb{P}$  in  $N$  do
6:     if  $\mathbb{P}.I \cap [l_q, u_q] \neq \emptyset$  then ▷ the interval  $\mathbb{P}$  covered
7:        $I^* \leftarrow \mathbb{P}.I \cap [l_q, u_q]$ 
8:        $\beta \leftarrow \{x \in I^* \mid \mathbb{P}'(x) = 0\}$  ▷ zero derivative points
9:        $\tilde{A}_{max} \leftarrow \max(\tilde{A}_{max}, \max_{x \in \beta} \mathbb{P}(x), \mathbb{P}(I^*.l), \mathbb{P}(I^*.u))$ 
10: if  $N$  is root node and  $Q_{type} = Q_{rel}$  then
11:   if  $\tilde{A}_{max}$  fails the error condition of Lemma 5.4 then
12:      $\tilde{A}_{max} \leftarrow$  perform refinement on  $\mathcal{D}$  ▷ Section 3.2.2
13: return  $A$ 

```

Table 2: Number of arithmetic operations for calculating zero derivative points

degree	1	2	3	4	5
operations	0	2	up to 18	up to 261	up to 1612

5.3 Tuning deg and δ

We discuss the effect of our index parameters (e.g., deg , δ) on the query response time, and then examine how to tune them.

How to tune the degree deg ?

The exact function $F(k)$ could be approximated by different polynomial functions (with different degrees). For instance, in Figure 8, the exact function $F(k)$ could be approximated by either of the following functions (within the deviation threshold δ): (i) a piecewise function $G(k)$ with four pieces of degree-1 functions,

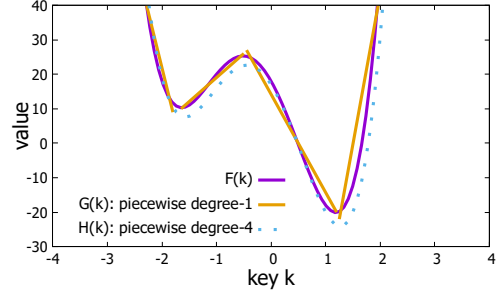


Figure 8: An example of degree selection

or (ii) a single-piece function $H(k)$ of degree-4. Based on our experimental findings (in Section 7.2.1), we recommend to set the degree to 2 or 3. In general, one could generate a random workload of queries to measure the performance of an index, and then test the performance of index structures at different degrees (e.g., from 1 to 4).

As a remark, it is not practical to use an arbitrarily large degree, due to the limited precision of numeric data types in both the linear programming solver and the programming language [1, 2]. For example, IBM CPLEX uses κ (kappa) as a statistical measurement of numerical difficulties. In our experiments, the κ value of a degree-4 polynomial ($1E+10$) is much higher than that of a degree-1 polynomial ($1E+05$).

How to tune δ ?

The tuning of δ depends on the most frequent query type used in the given application. For Q_{abs} (i.e., Problem 1), if all users share the same absolute error threshold ϵ_{abs} , then it is used to derive the value of δ , according to Lemmas 5.1 and 5.3. Otherwise, we could select the value of δ such that it can satisfy the error requirements for the majority of users (e.g., 80%).

For Q_{rel} (i.e., Problem 2), the processing includes three phases: index search, function evaluation, and refinement (cf. Algorithm 2, 3). A large δ leads to fast index search but high refinement probability. In contrast, a small δ leads to slow index search but low refinement probability. Observe that refinement is often more expensive than index search. We recommend to pick a small δ such that the majority of users can avoid the refinement phase. In our experiments, we examine different δ value (e.g., 25, 50, 100, 200, 500, and 1000) to identify the best setting for query response time.

6 EXTENSIONS: QUERIES WITH TWO KEYS

In previous sections, we mainly focus on range aggregate queries, in which each element only contains one single key (cf. Definition 3.1). However, existing works [27, 28, 32, 60] also support range aggregate queries with two keys for each element. In this section, we discuss how to extend our techniques in this setting (cf. Definition 6.1). Due to the space limit, we only consider the COUNT query.

Definition 6.1. Given \mathcal{D} as a set of elements (u, v, w) , where u , v and w are the first key, second key and the measure respectively, and the ranges of keys are $[l_q^{(1)}, u_q^{(1)}]$ for u and $[l_q^{(2)}, u_q^{(2)}]$ for v , we define the COUNT query as:

$$R_{\text{count}}(\mathcal{D}, [l_q^{(1)}, u_q^{(1)}], [l_q^{(2)}, u_q^{(2)}]) = \text{COUNT}(\sigma_{u \in [l_q^{(1)}, u_q^{(1)}], v \in [l_q^{(2)}, u_q^{(2)}]}(\mathcal{D}))$$

We build the following key-cumulative function to represent the surface (cf. Figure 9), which is formally stated in Definition 6.2.

Definition 6.2. The key-cumulative function with two keys for COUNT query is defined as $CF_{\text{count}}(u, v)$, where:

$$CF_{\text{count}}(u, v) = R_{\text{count}}(\mathcal{D}[-\infty, u][-\infty, v]) \quad (18)$$

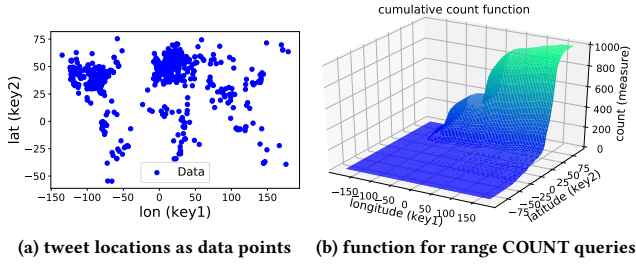


Figure 9: Tweet locations, 2-dimensional keys: discrete data points vs. continuous function

Therefore, we can solve the COUNT query with the following equation.

$$R_{\text{count}}(\mathcal{D}[l_q^{(1)}, u_q^{(1)}][l_q^{(2)}, u_q^{(2)}]) = CF_{\text{count}}(u_q^{(1)}, u_q^{(2)}) - CF_{\text{count}}(l_q^{(1)}, u_q^{(2)}) - CF_{\text{count}}(u_q^{(1)}, l_q^{(2)}) + CF_{\text{count}}(l_q^{(1)}, l_q^{(2)})$$

Then, we follow the similar idea in Section 4.1 and utilize the polynomial surface $\mathbb{P}(u, v)$ to approximate the key cumulative function $CF_{\text{count}}(u, v)$ with two keys, where:

$$\mathbb{P}(u, v) = \sum_{i=0}^{\deg} \sum_{j=0}^{\deg} a_{ij} u^i v^j$$

By replacing $F(k_i)$ and $\mathbb{P}(k_i)$ in Equation 9 with $F(u_i, v_i)$ and $\mathbb{P}(u_i, v_i)$ respectively, we can obtain the similar linear programming problem for obtaining the best parameters a_{ij} . However, unlike the one-dimensional case, it takes at least $O(n^2)$ to obtain the minimum number of segmentations by using the GS method (cf. Section 4.2.1), which is infeasible even for small-scale dataset (e.g., 10000 points). As such, we propose a heuristics-based solution that performs quad-tree-like segmentations. As illustrated in Figure 10, when a region does not fulfill the error guarantee δ (e.g., white rectangles), it is decomposed into four smaller regions. This procedure terminates when all regions satisfy the error guarantee δ .

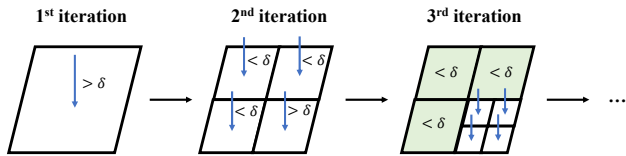


Figure 10: Quad-tree based approach for obtaining the segmentation

After building this index structure PolyFit, we utilize a similar approach in Section 5 to answer range aggregate queries with theoretical guarantee (cf. Lemmas 6.3 and 6.4).

Given the query range $[l_q^{(1)}, u_q^{(1)}]$ for u and $[l_q^{(2)}, u_q^{(2)}]$ for v , we propose to compute the approximate result as:

$$\tilde{A}_{\text{count}} = \mathbb{P}_{I_{uu}}(u_q^{(1)}, u_q^{(2)}) - \mathbb{P}_{I_{lu}}(l_q^{(1)}, u_q^{(2)}) - \mathbb{P}_{I_{ul}}(u_q^{(1)}, l_q^{(2)}) + \mathbb{P}_{I_{ll}}(l_q^{(1)}, l_q^{(2)}) \quad (19)$$

where I_{uu} , I_{lu} , I_{ul} , and I_{ll} denote the coverage regions of \mathbb{P} that $(u_q^{(1)}, u_q^{(2)})$, $(l_q^{(1)}, u_q^{(2)})$, $(u_q^{(1)}, l_q^{(2)})$, and $(l_q^{(1)}, l_q^{(2)})$ overlap respectively. These regions could be efficiently found with the same quad-tree index used in construction.

LEMMA 6.3. *If we set $\delta = \frac{\varepsilon_{\text{abs}}}{4}$, then A satisfies the absolute error guarantee ε_{abs} .*

LEMMA 6.4. *If $A_{\text{rel}} \geq 4\delta(1 + \frac{1}{\varepsilon_{\text{rel}}})$, then A satisfies the relative error guarantee ε_{rel} .*

The proofs of Lemma 6.3 and 6.4 are similar to those of Lemmas 5.1 and 5.2 respectively.

7 EXPERIMENTAL EVALUATION

We introduce the experimental setting in Section 7.1. Then, we investigate the performance of PolyFit in Section 7.2. Next, we compare PolyFit and error-bounded competitors on real datasets in Section 7.3. Lastly, we compare the response time of PolyFit with other heuristic methods in Section 7.4.

7.1 Experimental Setting

We use three real large-scale datasets (0.9M to 100M records) to evaluate the performance. They are summarized in Table 3. For each dataset, we randomly generate 1000 queries. In the single-key case, we randomly choose two keys in the datasets as the start and end points of each query interval. In the two-key case, we randomly sample rectangles from the dataset as query regions. In our experiments, we only focus on COUNT and MAX queries. Nevertheless, our methods are readily applicable to SUM and MIN queries.

Table 3: Datasets

Name	Size	Selected key(s)	Selected measure	Aggregate function
HKI [3]	0.9M	timestamp	index value	MAX
TWEET [15]	1M	latitude	# of tweets	COUNT
OSM [5]	100M	latitude, longitude	# of records	COUNT

Table 4 summarizes different methods for supporting range aggregate queries. We classify these methods based on five features, which are listed as follows.

- Can it provide absolute error guarantee (cf. Problem 1 (Q_{abs}))?
- Can it provide the relative error guarantee (cf. Problem 2 (Q_{rel}))?
- Can it support queries with two keys (cf. Section 6)?
- Can it support COUNT query?
- Can it support MAX query?

Table 4: Methods for range aggregate queries

✓ Directly support Δ Extend to support × Cannot support

Method	Q_{abs}	Q_{rel}	2 keys	COUNT	MAX
aR-tree [54]	✓	✓	✓	✓	✓
MRTree [40]	✓	✓	✓	✓	✓
RMI [39]	Δ	Δ	×	✓	×
FITing-tree [23]	Δ	Δ	×	✓	×
PGM [22]	Δ	Δ	×	✓	×
PolyFit (ours)	✓	✓	✓	✓	✓
Hist [62]	×	×	×	✓	×
S-tree [4]	×	×	×	✓	×
S2 [30]	×	×	✓	✓	×
VerdictDB [55]	×	×	✓	✓	×
DBest [48]	×	×	✓	✓	×
PLATO [45]	×	×	×	✓	×

We first introduce the methods that can satisfy deterministic error guarantees (i.e., those with ✓ or Δ in the Q_{abs} and Q_{rel} columns in Table 4). The aR-tree [54] is a traditional tree-based method for answering exact COUNT and MAX queries. The MRTree

[40] extends the aR-tree by utilizing progressive lower and upper bounds to answer approximate COUNT and MAX queries with error guarantees. In addition, both the aR-tree and the MRTree can support the range aggregate queries with two keys. With simple modifications, learned-index methods, including RMI [39], FITing-tree [23], and PGM [22], can be extended to support range aggregate queries with both absolute error and relative error guarantees. However, they are unable to support queries with two keys and the MAX query. Due to the space limitation, we cover the discussion of the modifications and parameter tuning in our technical report (cf. Appendix in [43]). PolyFit can support all these five features. By default, we follow Lemmas 5.1, 5.3, and 6.3 to set the δ values in Problem 1 (Q_{abs}), for different absolute error threshold ϵ_{abs} . In addition, we adopt $\delta = 100$ in PolyFit for the experiments with two keys in Problem 2 (Q_{rel}).

We then discuss the methods that are unable to fulfill the deterministic error guarantee (i.e., the methods with \times in the Q_{abs} and Q_{rel} columns in Table 4). Hist [62] adopts the entropy-based histogram for answering the COUNT query. The S-tree prebuilds the STX B-tree [4] on top of a sampled subset of each dataset. S2 [30] and VerdictDB [55] are the sampling-based approaches which can only provide probabilistic error guarantee. By default, we set the probability as 0.9 in our experiments. Both DBest [48] and PLATO [45] are the state-of-the-art methods in approximate query processing and time series database respectively, that can be also adapted to answer approximate range aggregate queries. Since these methods cannot provide deterministic error guarantees, we regard them as heuristic methods.

We implemented all methods in C++ and conducted experiments on an Intel Core i7-8700 3.2GHz PC using WSL (Windows 10 Subsystem for Linux).

7.2 PolyFit Tuning and Construction Time

In this section, we investigate two research questions for our method PolyFit, namely (1) how does the degree deg affect the query response time of PolyFit? (2) how do parameters affect the construction time of PolyFit?

7.2.1 Effect of deg on the query response time. Recall that we need to select the degree deg in order to build PolyFit. It is thus important to understand how this parameter affects the query response time. Here, we use the form PolyFit- deg to represent the degree deg of PolyFit. Figure 11 shows the trends for the query response time for both COUNT (one key and two keys) and MAX (one key) queries, using the absolute error threshold $\epsilon_{abs} = 100$. When we choose a larger degree deg , the polynomial function can provide better approximation for $F(k)$, and thus reduce the index size, which can reduce the response time for each query. However, the larger the degree deg , the larger the computation time for each node in PolyFit. Therefore, we can find that the response time increases (e.g., $deg = 3$ and 4 in Figure 11a), once we utilize the high degree deg . By default, we choose $deg = 2, 3$, and 3 for the COUNT query with single key, COUNT query with two keys, and MAX query, respectively in subsequent experiments.

7.2.2 Effect of parameters on the construction time. We first test how the construction time changes across different dataset sizes. Here, we adopt the default degrees, i.e., $deg = 2$ and $deg = 3$, for the polynomial functions in the COUNT query with single key and two keys respectively. In Figure 12, PolyFit only takes less than 150s and 2500s (with default deg) in the construction stage with 1 million (TWEET) and 30 million records (OSM)

respectively, which are acceptable in practice as the datasets are normally static in data analytics tasks.

Then, we further examine the construction time for PolyFit, varying the highest degree deg from 1 to 4 in the polynomial function (cf. Figure 13). Since the polynomial function with higher degree can produce error guarantee for longer interval I , i.e., $E(I) \leq \delta$, GS method needs to call the LP solver with longer intervals (cf. line 4 in Algorithm 1), which can increase the construction time for using the polynomial function with higher degree deg .

7.3 Comparisons with Error-Bounded Methods

In this section, we test the response time of different methods that can fulfill the absolute and relative error guarantees. Here, we adopt the default settings for these methods (cf. Section 7.1) and use the datasets HKI, TWEET and OSM for testing the performance of COUNT (single key), MAX (single key) and COUNT (two keys) queries respectively. For Problem 1 (Q_{abs}), we fix the absolute error $\epsilon_{abs} = 100$ and $\epsilon_{abs} = 200$ for the experiments with one key and two keys respectively. For Problem 2 (Q_{rel}), we fix the relative error $\epsilon_{rel} = 0.01$. Table 5 shows the response time of different methods. Observe that PolyFit achieves the best performance for different types of queries. For COUNT query with two keys, PolyFit can achieve a speedup of at least two-order-of-magnitude over the existing methods.

Table 5: Response time (nanoseconds) for all methods with error guarantees

Error guarantee	1 (Q_{abs})			2 (Q_{rel})		
Query type	COUNT	MAX	COUNT	COUNT	MAX	COUNT
# of keys	1	1	2	1	1	2
aR-tree	590	3592	357457	590	3592	357457
MRTree	565	182	385391	335	138	98919
RMI	568	n/a	n/a	579	n/a	n/a
FITing-tree	135	n/a	n/a	147	n/a	n/a
PGM	104	n/a	n/a	118	n/a	n/a
Polyfit	68	63	5274	79	65	5299

Sensitivity of ϵ_{abs} for COUNT query. We investigate how the absolute error ϵ_{abs} affects the response time of different methods. For the COUNT query with single key, we choose five absolute error values for testing, which are 100, 200, 400, 1000, and 2000. Observe from Figure 14a, since both the methods PolyFit, FITing-tree, and PGM can provide the more compact index structures for the datasets, all these methods can significantly improve the efficiency performance, compared with the traditional index structures, i.e., the aR-tree and the MRTree. In addition, due to the better approximation with nonlinear polynomial function ($deg = 2$), PolyFit can achieve 1.33x to 6x speedups, over the existing learned-index structures, including RMI, FITing-tree, and PGM. For the COUNT query with two keys, we choose 200, 400, 800, 2000, and 4000 as the absolute error values for testing. Since the state-of-the-art learned index structures (RMI, FITing-tree, and PGM) can only support queries with a single key, we omit these methods in this experiment. Figure 14b shows that PolyFit achieves at least one-order-of-magnitude speedups compared with the existing methods (aR-tree and MRTree), which is due to its compact index structure.

Sensitivity of ϵ_{rel} for COUNT query. We proceed to test how the relative error ϵ_{rel} affects the response time of different methods. In this experiment, we choose five relative error values,

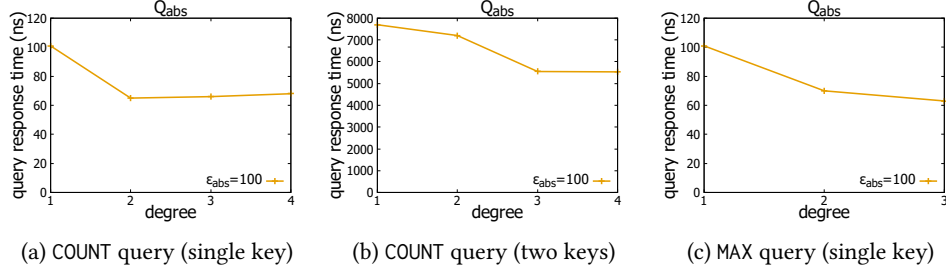


Figure 11: Running time for COUNT (single key), COUNT (two keys), and MAX queries on TWEET, OSM, and HKI datasets respectively, varying the degree deg of PolyFit

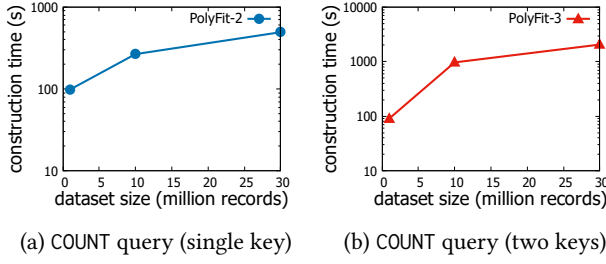


Figure 12: Construction time of PolyFit for COUNT query with single key and two keys (using OSM dataset for both settings), varying the dataset size

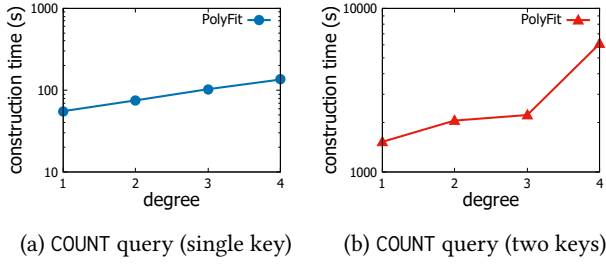


Figure 13: Construction time of PolyFit for COUNT query with single key (using TWEET dataset) and two keys (using OSM dataset), varying the degree deg

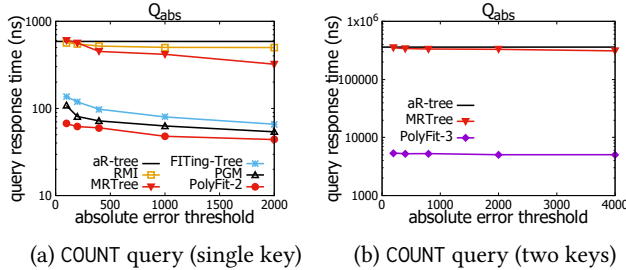


Figure 14: Response time for COUNT query in TWEET dataset (for single key) and OSM dataset (for two keys), varying the absolute error ϵ_{abs}

which are 0.005, 0.01, 0.05, 0.1, and 0.2. Based on the more compact index structure of PolyFit, our method PolyFit can achieve better efficiency performance, compared with the existing methods (cf. Figure 15a). For the COUNT query with two keys, PolyFit can significantly outperform the existing methods, i.e., the aR-tree and the MRTree, by at least one-order-of-magnitude (cf. Figure 15b).

Sensitivity of ϵ_{abs} and ϵ_{rel} for MAX query. In this experiment, we proceed to investigate how the absolute error ϵ_{abs} and relative error ϵ_{rel} affect the efficiency performance of different

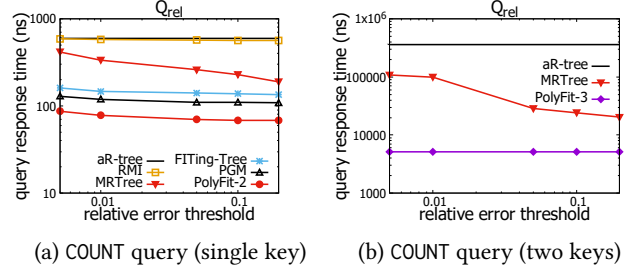


Figure 15: Response time for COUNT query in TWEET dataset (for single key) and OSM dataset (for two keys), varying the relative error ϵ_{rel}

methods. Observe from Figure 16, our method PolyFit can achieve at least 2x speedup, compared with other methods, even though the selected error is small.

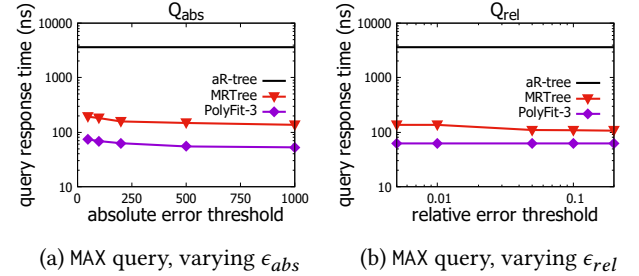


Figure 16: Response time for MAX query in HKI dataset

Sensitivity of the selectivity for COUNT query. We further test the response time of different methods, varying the selectivity of the COUNT query. Observe from Figure 17, once we increase the selectivity of the COUNT query (i.e., each query can cover a larger region), the query response time can normally increase in different methods. Since all methods for COUNT query with single key have the logarithmic time complexity, they are not sensitive to the selectivity (cf. Figure 17a). Unlike the single key case, both the existing methods aR-tree and MRTree are sensitive to the selectivity, compared with our method PolyFit (cf. Figure 17b).

In both cases, PolyFit can achieve better performance across different selectivities. As a remark, since the methods MRTree, aR-tree, and RMI always provide inferior efficiency performance in the single key case (cf. Figures 14a, 15a and 17a), compared with Fitting-Tree, PGM and PolyFit, we omit their results in subsequent experiments.

Scalability to the dataset size. We proceed to test how the dataset size affects the efficiency performance of both PolyFit and other methods. In this experiment, we choose the largest dataset OSM (with 100M) for testing. Here, we focus on solving the Problem 1 (Q_{abs}) for COUNT query, in which we adopt the

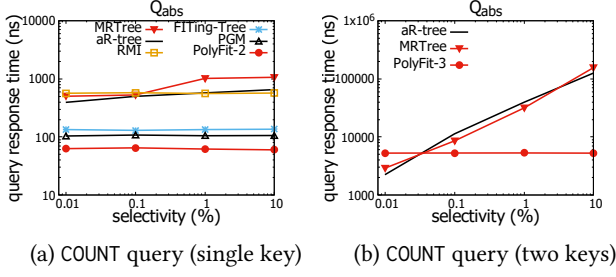


Figure 17: Response time for COUNT query in TWEET dataset (for single key) and OSM dataset (for two keys), varying the selectivity of the query

default absolute errors, i.e., $\epsilon_{abs} = 100$ and $\epsilon_{abs} = 200$ for the cases in single key and two keys respectively, and choose the latitude attribute as key. To conduct this experiment, we choose five dataset sizes, which are 1M, 10M, 30M, and 100M. Observe from Figure 18, PolyFit scales well with the dataset size and outperforms other methods.

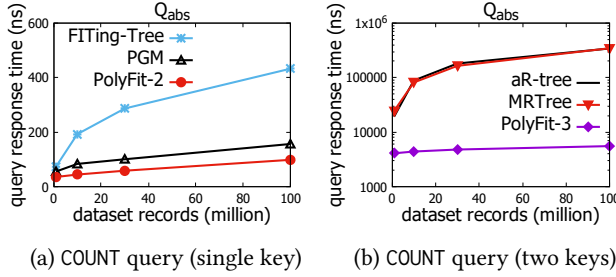


Figure 18: Response time for COUNT query in OSM dataset, varying the dataset size

Trade-off between the query response time and index size. We proceed to investigate the trade-off between the query response time and index size of different indexing methods. To conduct this experiment, we focus on Problem 2 (Q_{rel}) and choose 25, 50, 100, 200, 500, and 1000 as the parameter δ for testing. In Figure 19, we can observe that the smaller the δ , the larger the index size and query response time. The reason is the smaller δ values lead to more leaf nodes in index structures in different methods (e.g., more intervals are generated by GS method (cf. Algorithm 1) in PolyFit). On the other hand, if δ is too large, it is easier for the online query to violate the error condition for Q_{rel} (i.e., Lemma 5.2), and thus the query response time can also be larger. As such, all curves in Figure 19 resemble the “C”-shape. In general, our method PolyFit-2 offers better trade-off compared with other methods.

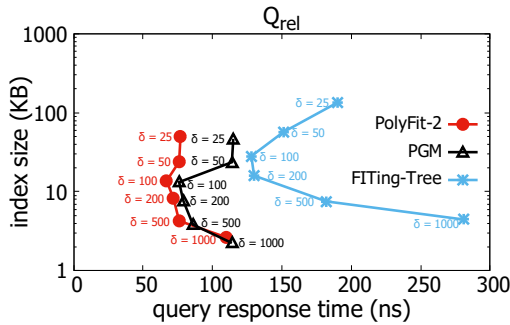


Figure 19: Trade-off between the query response time and index size of COUNT query (single key) in TWEET dataset, for Q_{rel} with $\epsilon_{rel} = 0.01$, using $\delta = 25, 50, 100, 200, 500$, and 1000

7.4 Comparisons with Heuristic Methods

We compare the response time of PolyFit with other heuristic methods, which cannot fulfill deterministic error guarantees, i.e., Q_{abs} (cf. Problem 1) and Q_{rel} (cf. Problem 2). In this experiment, we adopt the default setting for the method PLATO [45], vary the bin size for the method Hist and vary the sampling size for the sampling-based methods, including S-tree, S2, VerdictDB, and DBest. Since S2 cannot achieve less than 100000ns query response time with 10% measured relative error, we omit the result of S2 in Figure 20a. In addition, we only report the results of the heuristic methods DBest and VerdictDB in Figure 20b, as the other heuristic methods cannot support COUNT query with two keys (cf. Table 4). In these two figures, our method PolyFit yields the smallest query response time with similar relative error.

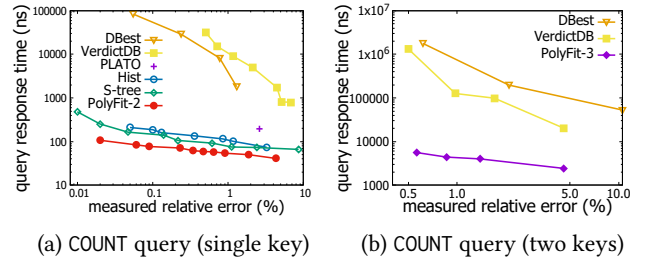


Figure 20: Response time between PolyFit and the heuristic methods for COUNT query with single key and two keys in TWEET and OSM datasets respectively

8 CONCLUSION

In this paper, we study the range aggregate queries with two types of approximate guarantees, which are (1) absolute error guarantee (cf. Problem 1 (Q_{abs})) and (2) relative error guarantee (cf. Problem 2 (Q_{rel})). Unlike the existing methods, our work can efficiently support the most commonly used range aggregate queries (SUM, COUNT, MIN, MAX), fulfill the error guarantees and support the setting of two keys.

In order to improve the efficiency for these queries, we utilize several polynomial functions to fit the data points and then build the compact index structure PolyFit on top of these polynomial functions. Our experiment results show that PolyFit can achieve significant speedups compared with existing learned-index methods and other traditional exact/ approximate methods in different query types. In particular, we can achieve at most 5μs query response time in the dataset with 30 million records, which cannot be achieved by the state-of-the-art methods.

In the future, we plan to further develop advanced techniques to improve the efficiency performance for constructing PolyFit, in order to handle the update of records in large-scale datasets. In addition, we will also extend our methods to support other fundamental operations in analytic databases, including standard deviation, median etc. Moreover, we also plan to investigate how to utilize the idea of PolyFit to further improve the efficiency performance for other types of statistics and machine learning models, e.g., kernel density estimation, kernel clustering, and support vector machines.

REFERENCES

- [1] Cplex performance tuning for linear programs. <https://www.ibm.com/support/pages/node/397127#Item4>.
- [2] Diagnosing ill conditioning. <https://www.ibm.com/support/pages/node/397063>.
- [3] Hong kong 40 index 2018. <https://www.dukascopy.com/swiss/english/marketwatch/historical/>. [Online; accessed 20-Dec-2019].

- [4] STX B+ Tree. <https://panthema.net/2007/stx-btree/>. [Online; accessed 11-Jan-2019].
- [5] OpenStreetMap dataset. <https://registry.opendata.aws/osm/>, 2019. [Online; accessed 19-May-2019].
- [6] A. Aboulmaga and S. Chaudhuri. Self-tuning histograms: Building histograms without looking at data. In *SIGMOD*, pages 181–192, 1999.
- [7] S. S. Abraham Silberschatz, Henry F. Korth. *Database System Concepts (6th Edition)*. McGraw-Hill, 2011.
- [8] S. Agarwal, B. Mozafari, A. Panda, H. Milner, S. Madden, and I. Stoica. Blinkdb: queries with bounded errors and bounded response times on very large data. In *EuroSys*, pages 29–42, 2013.
- [9] C. Anagnostopoulos and P. Triantafillou. Learning to accurately count with query-driven predictive analytics. In *BigData*, pages 14–23, 2015.
- [10] M. Armbrust, R. S. Xin, C. Lian, Y. Huai, D. Liu, J. K. Bradley, X. Meng, T. Kaftan, M. J. Franklin, A. Ghodsi, et al. Spark SQL: Relational data processing in Spark. In *SIGMOD*, pages 1383–1394, 2015.
- [11] D. Bartholomew. *MariaDB cookbook*. Packt Publishing Ltd, 2014.
- [12] S. M. Beitzel, E. C. Jensen, A. Chowdhury, D. Grossman, and O. Frieder. Hourly analysis of a very large topically categorized web query log. In *SIGIR*, pages 321–328, 2004.
- [13] J. L. Bentley and A. C. Yao. An almost optimal algorithm for unbounded searching. *Inf. Process. Lett.*, 5(3):82–87, 1976.
- [14] K. Chan and A. W. Fu. Efficient time series matching by wavelets. In *ICDE*, pages 126–133, 1999.
- [15] L. Chen, G. Cong, X. Cao, and K.-L. Tan. Temporal spatial-keyword top-k publish/subscribe. In *ICDE*, pages 255–266, 2015.
- [16] T. Condie, N. Conway, P. Alvaro, J. M. Hellerstein, J. Gerth, J. Talbot, K. Elmelegy, and R. Sears. Online aggregation and continuous query support in mapreduce. In *SIGMOD*, pages 1115–1118, 2010.
- [17] T. H. Cormen, C. Stein, R. L. Rivest, and C. E. Leiserson. *Introduction to Algorithms*. McGraw-Hill Higher Education, 2nd edition, 2001.
- [18] M. de Berg, O. Cheong, M. J. van Kreveld, and M. H. Overmars. *Computational geometry: algorithms and applications, 3rd Edition*. Springer, 2008.
- [19] K. Delaney. *Inside Microsoft SQL Server 2000*. Microsoft Press, 2000.
- [20] A. Eldawy, M. F. Mokbel, S. Al-Harthi, A. Alzaidey, K. Tarek, and S. Ghani. SHAHED: A mapreduce-based system for querying and visualizing spatio-temporal satellite data. In *ICDE*, pages 1585–1596, 2015.
- [21] C. Faloutsos, M. Ranganathan, and Y. Manolopoulos. Fast subsequence matching in time-series databases. In *SIGMOD*, pages 419–429, 1994.
- [22] P. Ferragina and G. Vinciguerra. The PGM-index: a fully-dynamic compressed learned index with provable worst-case bounds. *Proc. VLDB Endow.*, 13(8):1162–1175, 2020.
- [23] A. Galakatos, M. Markovitch, C. Binnig, R. Fonseca, and T. Kraska. Fitting-tree: A data-aware index structure. In *SIGMOD*, pages 1189–1206, 2019.
- [24] M. Garofalakis and P. B. Gibbons. Wavelet synopses with error guarantees. In *SIGMOD*, pages 476–487, 2002.
- [25] M. N. Garofalakis and P. B. Gibbons. Probabilistic wavelet synopses. *ACM Trans. Database Syst.*, 29:43–90, 2004.
- [26] J. L. Gearhart, K. L. Adair, R. J. Detry, J. D. Durfee, K. A. Jones, and N. Martin. Comparison of open-source linear programming solvers. *Sandia National Laboratories, SAND2013-8847*, 2013.
- [27] D. Gunopulos, G. Kollios, V. J. Tsotras, and C. Domeniconi. Approximating multi-dimensional aggregate range queries over real attributes. In *SIGMOD*, pages 463–474, 2000.
- [28] D. Gunopulos, G. Kollios, V. J. Tsotras, and C. Domeniconi. Selectivity estimators for multidimensional range queries over real attributes. *VLDBJ*, 14(2):137–154, 2005.
- [29] P. J. Haas, J. F. Naughton, and A. N. Swami. On the relative cost of sampling for join selectivity estimation. In *PODS*, pages 14–24, 1994.
- [30] P. J. Haas and A. N. Swami. Sequential sampling procedures for query size estimation. In *SIGMOD*, pages 341–350, 1992.
- [31] S. Han, H. Wang, J. Wan, and J. Li. An iterative scheme for leverage-based approximate aggregation. In *ICDE*, pages 494–505, 2019.
- [32] M. Heimel, M. Kiefer, and V. Markl. Self-tuning, gpu-accelerated kernel density models for multidimensional selectivity estimation. In *SIGMOD*, pages 1477–1492, 2015.
- [33] C.-T. Ho, R. Agrawal, N. Megiddo, and R. Srikant. Range queries in olap data cubes. In *SIGMOD*, pages 73–88, 1997.
- [34] I. F. Ilyas, V. Markl, P. Haas, P. Brown, and A. Aboulmaga. Cords: automatic discovery of correlations and soft functional dependencies. In *SIGMOD*, pages 647–658, 2004.
- [35] S. K. Jensen, T. B. Pedersen, and C. Thomsen. Modelardb: modular model-based time series management with spark and cassandra. *PVLDB*, 11(11):1688–1701, 2018.
- [36] E. J. Keogh. Fast similarity search in the presence of longitudinal scaling in time series databases. In *ICITAI*, pages 578–584, 1997.
- [37] E. J. Keogh, S. Chu, D. M. Hart, and M. J. Pazzani. An online algorithm for segmenting time series. In *ICDM*, pages 289–296, 2001.
- [38] E. J. Keogh and M. J. Pazzani. An enhanced representation of time series which allows fast and accurate classification, clustering and relevance feedback. In *KDD*, pages 239–243, 1998.
- [39] T. Kraska, A. Beutel, E. H. Chi, J. Dean, and N. Polyzotis. The case for learned index structures. In *SIGMOD*, pages 489–504, 2018.
- [40] I. Lazaridis and S. Mehrotra. Progressive approximate aggregate queries with a multi-resolution tree structure. In *SIGMOD*, pages 401–412, 2001.
- [41] Y. T. Lee and A. Sidford. Efficient inverse maintenance and faster algorithms for linear programming. In *FOCS*, pages 230–249, 2015.
- [42] D. Leenaerts and W. van Bokhoven. *Piecewise Linear Modeling and Analysis*. Springer US, 2013.
- [43] Z. Li, T. N. Chan, M. L. Yiu, and C. S. Jensen. Polyfit: Polynomial-based indexing approach for fast approximate range aggregate queries. *CoRR*, abs/2003.08031, 2020.
- [44] L. Lim, M. Wang, and J. S. Vitter. Sash: A self-adaptive histogram set for dynamically changing workloads. In *VLDB*, pages 369–380, 2003.
- [45] C. Lin, E. Boursier, and Y. Papakonstantinou. Plato: approximate analytics over compressed time series with tight deterministic error guarantees. *VLDB*, 13(7):1105–1118, 2020.
- [46] R. J. Lipton, J. F. Naughton, and D. A. Schneider. Practical selectivity estimation through adaptive sampling. In *SIGMOD*, pages 1–11, 1990.
- [47] C. A. Lynch. Selectivity estimation and query optimization in large databases with highly skewed distribution of column values. In *VLDB*, pages 240–251, 1988.
- [48] Q. Ma and P. Triantafillou. Dbest: Revisiting approximate query processing engines with machine learning models. In *SIGMOD*, pages 1553–1570, 2019.
- [49] A. Marcus, M. S. Bernstein, O. Badar, D. R. Karger, S. Madden, and R. C. Miller. Processing and visualizing the data in tweets. *SIGMOD Record*, 40(4):21–27, 2011.
- [50] V. Markl, P. J. Haas, M. Kutsch, N. Megiddo, U. Srivastava, and T. M. Tran. Consistent selectivity estimation via maximum entropy. *VLDBJ*, 16(1):55–76, 2007.
- [51] B. Momjian. *PostgreSQL: introduction and concepts*, volume 192. Addison-Wesley New York, 2001.
- [52] M. Muralikrishna and D. J. DeWitt. Equi-depth multidimensional histograms. In *SIGMOD*, pages 28–36, 1988.
- [53] T. Palpanas, M. Vlachos, E. J. Keogh, and D. Gunopulos. Streaming time series summarization using user-defined amnesic functions. *TKDE*, 20(7):992–1006, 2008.
- [54] D. Papadias, P. Kalnis, J. Zhang, and Y. Tao. Efficient OLAP operations in spatial data warehouses. In *SSTD*, pages 443–459, 2001.
- [55] Y. Park, B. Mozafari, J. Sorenson, and J. Wang. VerdictDB: Universalizing approximate query processing. In *SIGMOD*, pages 1461–1476, 2018.
- [56] Y. Park, S. Zhong, and B. Mozafari. Quicksel: Quick selectivity learning with mixture models. In *SIGMOD, June 14–19, 2020*, pages 1017–1033, 2020.
- [57] I. Popivanov and R. J. Miller. Similarity search over time-series data using wavelets. In *ICDE*, pages 212–221, 2002.
- [58] D. Rafiei. On similarity-based queries for time series data. In *ICDE*, pages 410–417, 1999.
- [59] C. Ré and D. Suciu. Understanding cardinality estimation using entropy maximization. In *PODS*, pages 53–64, 2010.
- [60] M. Riondato, M. Akdere, U. Çetintemel, S. B. Zdonik, and E. Upfal. The vc-dimension of sql queries and selectivity estimation through sampling. In *ECML PKDD*, pages 661–676, 2011.
- [61] I. N. Stewart. *Galois theory*. CRC Press, 2015.
- [62] H. To, K. Chiang, and C. Shahabi. Entropy-based histograms for selectivity estimation. In *CIKM*, pages 1939–1948, 2013.
- [63] J. S. Vitter and M. Wang. Approximate computation of multidimensional aggregates of sparse data using wavelets. In *SIGMOD*, pages 193–204, 1999.
- [64] H. Wang, X. Fu, J. Xu, and H. Lu. Learned index for spatial queries. In *MDM*, pages 569–574, 2019.
- [65] A. Wasay, X. Wei, N. Dayan, and S. Idreos. Data canopy: Accelerating exploratory statistical analysis. In *SIGMOD*, pages 557–572, 2017.
- [66] E. Wu and S. Madden. Scorpion: Explaining away outliers in aggregate queries. *PVLDB*, 6(8):553–564, 2013.
- [67] X. Yu, Y. Xia, A. Pavlo, D. Sanchez, L. Rudolph, and S. Devadas. Sundial: harmonizing concurrency control and caching in a distributed oltp database management system. *PVLDB*, 11(10):1289–1302, 2018.
- [68] X. Yun, G. Wu, G. Zhang, K. Li, and S. Wang. Fastraq: A fast approach to range-aggregate queries in big data environments. *IEEE Trans. Cloud Computing*, 3(2):206–218, 2015.

A APPENDIX

A.1 Approximate Range Aggregate Queries via Learn Index Methods

The learned index methods, including RMI [39], FITing-tree [23], and PGM [22], are originally designed for range and point queries. In order to support range aggregate queries, e.g., SUM and MAX, with both absolute error and relative error guarantees (cf. Problem 1 and Problem 2), we follow the same mechanism of these index structures to fit the curve of either $CF_{sum}(k)$ or $DF_{max}(k)$ cf. Equation 7. Instead of finding the exact result for either range query or point query, we utilize our querying methods (i.e., Lemma 5.1 to 5.4) to solve both Problem 1 and Problem 2.

A.2 Tuning the RMI

RMI [39] is a flexible learned index structure, which contains many parameters for tuning this index, including: (1) types of machine learning models, (2) the number of stages in RMI, (3) the number of models for each stage in RMI. Here, we adopt the TWEET dataset (cf. Table 3) to tune the parameters, so as to obtain the best performance for RMI.

A.2.1 Model Selection. In [39], they adopt the neural network (NN) with at most two hidden layers and linear regression (LR) for testing the performance. Table 6 summarizes the response time and measured relative error, using single model to fit $CF_{sum}(k)$ in TWEET dataset for approximate SUM query. Here, we use 1:X:Y:1 to represent the NN architecture with two hidden layers, i.e., X and Y neurons in the first and second hidden layers respectively, where the first and last one denote the input and output respectively. Similarly, we also use 1:X:1 to represent one hidden layer of the NN architecture.

Even though NN model can generally provide accurate fitting to the curve ($CF_{sum}(k)$ in this experiment), the response time can be much larger, compared with linear regression model. As an example, once we choose the shallow NN architecture 1:8:1, the response time can achieve more than 100ns, which can be worse than the performance of FITing-tree (cf. Table 5). Due to the inefficiency issue of highly non-linear NN model, we choose LR model for RMI.

Table 6: Comparison of Different Machine Learning Models

Model	NN architecture	Prediction time (ns)	Measured Relative error (%)
LR	n.a.	20	38
NN	1:4:1	119	24.1
NN	1:8:1	189	25.3
NN	1:16:1	275	25.3
NN	1:4:4:1	152	24.8
NN	1:8:8:1	347	21.4
NN	1:16:16:1	972	23.3

A.2.2 Tuning RMI Structure. RMI utilize multiple models (e.g., LR) to obtain the approximate searching position (cf. Figure 21). However, due to the large degree of flexibility for RMI, including the number of stages and the number of models for each stage in RMI, we only test some of the combinations for choosing the structure of models, i.e., RMI structure.

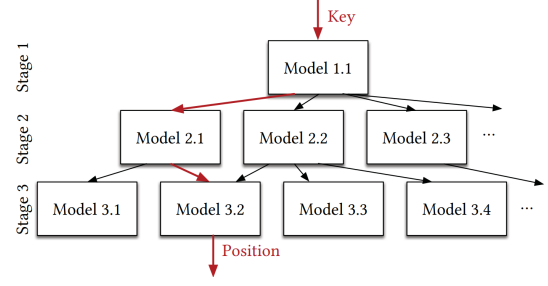


Figure 21: RMI structure (Cropped from [39])

Theoretically, RMI can provide better performance with the large number of models, in which RMI can consume more memory resources. As such, we restrict the number of models in the leaf level (stage 3 in Figure 21 as an example) of RMI to be approximately the same as PolyFit for the sake of fairness. Here, we use $1 \rightarrow 10 \rightarrow X$ to denote the three-stage RMI structure with one model in stage 1, ten models in stage 2 and X models in stage 3. Similarly, we also use $1 \rightarrow 10 \rightarrow 100 \rightarrow Y$ to denote the four-stage RMI structure. Here, we vary X from 100 to 1000 and vary Y from 100 to 1000, by increasing X/Y 100 each time. In our experiment, we find that the RMI structure $1 \rightarrow 10 \rightarrow 100 \rightarrow 1000$ can normally provide the smallest query response time, compared with other RMI structures. As such, we choose the RMI structure with $1 \rightarrow 10 \rightarrow 100 \rightarrow 1000$ and LR for each model in our experiments (cf. Section 7).